Published in Polyhedron 25 issue 18, 3617-3627, 2006
which should be used for any reference to this work

Synthesis, crystal structures and magnetic properties of trinuclear oxo-centered homo- and mixed-valence manganese pivalate complexes with imidazole (Im) and 1-methylimidazole (1-MeIm): $[Mn_3^{III}O(O_2CCMe_3)_6(Im)_3](Me_3CCO_2)\cdot 0.5Me_3CCO_2H$ and $[Mn_2^{III}Mn^{II}O(O_2CCMe_3)_6(1\text{-}MeIm)_3]$

Svetlana G. Baca [a,*], Helen Stoeckli-Evans [b], Christina Ambrus [c], Stanislav T. Malinovskii [a], Iurii Malaestean [a], Nicolae Gerbeleu [a], Silvio Decurtins [c,*]

[a] *Institute of Chemistry, Academy of Sciences of RM, MD-2028 Chisinau, Moldavia*
[b] *Institute of Microtechnology, University of Neuchâtel, CH-2009 Neuchâtel, Switzerland*
[c] *Department of Chemistry and Biochemistry, University of Berne, CH-3012 Berne, Switzerland*

Abstract

Two new μ_3-oxo-centered trinuclear manganese complexes, one of them a homo-valence $[Mn_3^{III}O(O_2CCMe_3)_6(Im)_3](Me_3CCO_2)\cdot 0.5Me_3CCO_2H$ (**1**) pivalate complex and the other a mixed-valence $[Mn_2^{III}Mn^{II}O(O_2CCMe_3)_6(1\text{-}MeIm)_3]$ (**2**) pivalate complex (where Im = imidazole, 1-MeIm = 1-methylimidazole), have been synthesized and characterized by IR spectroscopy, thermogravimetric analysis, X-ray crystallography and magnetochemistry. Complexes **1** and **2** are μ_3-oxo-trinuclear compounds with the three manganese atoms bridged by six pivalate groups. At each axial position there is an Im (**1**) or 1-MeIm (**2**) molecule. In both compounds, the manganese coordination geometry is slightly distorted octahedral, consisting of the oxygen of the central triangle, four oxygen atoms from bridging pivalate ligands, and a terminal Im or 1-MeIm nitrogen atom. The crystal packing of **1** involves hydrogen bonding between complex cations $[Mn_3O(Piv)_6(Im)_3]^+$ and outersphere pivalate ions, whereas in compound **2** interactions of the C–H$\cdots\pi$ type, formed by both the aromatic and methyl C–H groups of 1-MeIm molecules, are present. Magnetic studies reveal that both compounds represent antiferromagnetically coupled, spin-frustrated triangular systems exhibiting weak to moderate exchange coupling constants.

Keywords: Manganese complexes; Carboxylate complexes; Crystal structure; Magnetic properties

1. Introduction

In the past decade polynuclear manganese complexes have been of interest due to the remarkable magnetic properties of single-molecule magnets (for recent reviews see [1] and references therein) and their use as models of biological systems [2]. Much of the work in these areas has involved manganese carboxylates. A large number of polynuclear manganese carboxylate complexes has been prepared to date; many compounds are μ_3-oxo trinuclear complexes of the general formula $[Mn_3O(O_2CR)_6(L)_3]^z$ ($z = 1+, 0$) with a wide variety of both the bridging carboxylates and terminal ligands (L) [3–19]. However, interest in new trinuclear manganese carboxylates which can serve as both, precursors for higher nuclearity carboxylate complexes like Mn_9, Mn_{22}, etc., and as models for understanding the different magnetic interactions of manganese clusters, still remains.

* Corresponding authors. Tel.: +373 22 72 5490; fax: +373 22 73 9611 (S.G. Baca), Tel.: +41 31 631 4255; fax: +41 31 631 4399 (S. Decurtins).
E-mail addresses: sbaca_md@yahoo.com (S.G. Baca), silvio.decurtins@iac.unibe.ch (S. Decurtins).

We have been interested in the design, synthesis and investigation of polynuclear manganese complexes, especially based on pivalic acid [19–21]. In this paper, we report the synthesis, crystal structures and characterization of two new manganese pivalates, namely homo-valent $[Mn_3^{III}O\text{-}(O_2CCMe_3)_6(Im)_3](Me_3CCO_2) \cdot 0.5Me_3CCO_2H$ (**1**) and mixed-valent $[Mn_2^{III}Mn^{II}O(O_2CCMe_3)_6(1\text{-MeIm})_3]$ (**2**) (where Im = imidazole, 1-MeIm = 1-methylimidazole) complexes.

2. Experimental

2.1. Materials and methods

Starting materials were purchased from commercial sources and used without further purification. $[Mn_6O_2(O_2CCMe_3)_{10}(Me_3CCO_2H)_4]$ was prepared by the reported procedure [22]. The infrared spectra were recorded on a Perkin–Elmer Spectrum One spectrometer using KBr pellets in the region 4000–400 cm^{-1}. TG analyses were carried out on a Mettler-Toledo TA 50 in dry nitrogen (60 ml min^{-1}) at a heating rate of 5 °C min^{-1}.

2.2. Synthesis of complexes

2.2.1. Synthesis of $[Mn_3O(O_2CCMe_3)_6(Im)_3](Me_3CCO_2) \cdot 0.5Me_3CCO_2H$ (1)

Imidazole (1.25 g, 18.36 mmol) and pivalic acid (5.4 g, 52.89 mmol) were dissolved in water (4 ml) and stirred. Then, to this solution was added $MnCl_2 \cdot 4H_2O$ (0.8 g, 4.06 mmol) followed by adding solid $KMnO_4$ (0.25 g, 1.58 mmol) in small portions to give a brown homogeneous solution. Finally, this solution was heated at 60 °C for 1 h and then was left to stand overnight at r.t. The microcrystalline precipitate was filtered off, washed with hexane and dried in air. Single crystals suitable for X-ray analysis were obtained by recrystallization of **1** from MeCN. Yield (after recrystallization): 0.36 g (30%). *Anal.* Calc. for $C_{93}H_{160}Mn_6N_{12}O_{32}$: C, 48.82; H, 7.05; N, 7.35. Found: C, 48.65; H, 7.04; N, 7.38%. IR (KBr, cm^{-1}) 3159m, 3067m, 2960m, 2872m, 1609vs, 1570m, 1547m, 1510m, 1482s, 1458m, 1405s, 1370s, 1358s, 1329m, 1224s, 1148w, 1098w, 1069m, 958w, 938w, 895w, 836w, 786m, 751m, 655m, 625m, 598m, 562w.

2.2.2. Synthesis of $[Mn_3O(O_2CCMe_3)_6(1\text{-MeIm})_3]$ (2)

Complex $[Mn_6O_2(O_2CCMe_3)_{10}(Me_3CCO_2H)_4]$ (0.5 g, 0.28 mmol) and $KMnO_4$ (0.05 g, 0.31 mmol) were dissolved in 1-MeIm (2 ml). The mixture was heated at 90 °C for an hour and then the reaction was allowed to cool. After two days this mixture was extracted with diethyl ether. On the next day, from the diethyl ether extracts, crystals suitable for X-ray analysis formed. The crystals were filtered off and washed with cold diethyl ether. Yield: 0.27 g (31.03%). *Anal.* Calc. for $C_{84}H_{144}Mn_6N_{12}O_{26}$: C, 48.79; H, 7.02; N, 8.13. Found: C, 47.78; H, 6.80; N, 8.15%. IR (KBr, cm^{-1}) 3129m, 2958s, 2926sh, 2869sh, 1608br.vs, 1538m, 1526m, 1482s, 1457m, 1411vs, 1370s, 1358s, 1286w, 1227s, 1110s, 1024w, 956w, 932w, 893w, 831m, 788m, 762w, 733w, 695m, 656m, 615m, 599m.

2.3. X-ray crystallography

Diffraction data were collected at 153 K for **1** and **2** with a Stoe Mark II Imaging Plate Diffractometer using Mo Kα graphite-monochromated radiation. Crystallographic data and details of the refinement process are summarized in Table 1. The structures were solved by direct methods using the program SHELXS-97 [23]. Refinement and all further calculations were carried out using SHELXL-97 [24]. H-atoms were located from Fourier difference maps and refined isotropically; their thermal parameters were kept fixed with $U_{iso} = 1.5U_{eq}$ of their carrier O and N atoms. In both structures some of methyl groups in the pivalate fragments are disordered over two positions with occupancies 0.50 ± 0.10. Non-hydrogen atoms were refined anisotropically, using weighted full-matrix least-squares on F^2.

2.4. Magnetic measurements

Magnetic susceptibility and magnetization data of powdered samples of compounds **1** and **2** were collected on a MPMS Quantum Design SQUID magnetometer (XL-5) in the temperature range of 300–1.8 K and at applied magnetic fields up to 5 T. The samples were placed in a saran foil bag for compound **1** and in a gelatine capsule for compound **2**. A straw was used as the sample holder. Data were corrected for the experimentally determined diamagnetism of the sample holder and the diamagnetic contributions of the samples, which were estimated from Pascal's constants. The Levenberg–Marquardt least-squares fitting algorithm, in combination with MAGPACK [25], was used to model the experimental magnetic susceptibility and magnetization data.

3. Results and discussion

3.1. Synthesis and preliminary characterization

The reaction of manganese(II) chloride with $KMnO_4$, imidazole and an excess of pivalic acid in a small amount of water leads to the formation of $[Mn_3O(O_2CCMe_3)_6(Im)_3](Me_3CCO_2) \cdot 0.5Me_3CCO_2H$ (**1**). This method of preparing oxo-bridged manganese complexes by the oxidation of Mn(II) ions using MnO_4^- ions in the presence of carboxylate ligands and aromatic amines was first used by Lis for the synthesis of a dodecanuclear complex [26] and then largely developed by Christou et al. [6,27]; it is a very useful synthetic route to design Mn complexes with higher oxidation states (Mn^{III}, Mn^{IV}). Moreover, the largest manganese carboxylate cluster, a Mn_{30} complex [28], was also obtained from this type of comproportionation reaction. The synthesis of the mixed-valence compound $[Mn_3O(O_2CCMe_3)_6(1\text{-MeIm})_3]$ (**2**) was performed by the

Table 1
Crystal data and details of structure determination

	1	2
Empirical formula	$C_{93}H_{160}Mn_6N_{12}O_{32}$	$C_{42}H_{72}Mn_3N_6O_{13}$
Formula weight	2287.97	1033.87
Temperature (K)	153(2)	153(2)
Wavelength (Å)	0.71073	0.71073
Crystal size (mm)	$0.30 \times 0.30 \times 0.20$	$0.40 \times 0.20 \times 0.15$
Crystal system	monoclinic	monoclinic
Space group	$P2_1/n$	$P2_1$
a (Å)	13.6326(5)	19.685(2)
b (Å)	46.1720(16)	19.7203(12)
c (Å)	19.6917(8)	13.5507(13)
β (°)	100.175(3)	90.792(12)
V (Å^3)	12199.9(8)	5259.8(8)
Z	4	4
D_{calc} (g/cm^3)	1.246	1.306
μ (mm^{-1})	0.674	0.770
$F(000)$	4832	2180
θ Range for data collections (°)	1.14–25.10	2.07–25.96
Index ranges	$-16 \leqslant h \leqslant 16$, $-53 \leqslant k \leqslant 55$, $-23 \leqslant l \leqslant 23$	$-24 \leqslant h \leqslant 24$, $-24 \leqslant k \leqslant 23$, $-16 \leqslant l \leqslant 16$
Reflections measured	98816	41579
Independent reflections [R_{int}]	21524 [0.0757]	19412 [0.1037]
Data/restraints/parameters	21524/0/1557	19412/1/1211
Goodness-of-fit on F^2	0.884	0.745
Final R indices [$I > 2\sigma(I)$]	$R_1 = 0.0471$, $wR_2 = 0.1098$	$R_1 = 0.0509$, $wR_2 = 0.0856$
R indices (all data)	$R_1 = 0.0876$, $wR_2 = 0.1246$	$R_1 = 0.1238$, $wR_2 = 0.1019$
Largest difference peak and hole (e Å^{-3})	0.355 and −0.312	0.477 and −0.528

interaction of the hexanuclear mixed-valent $[Mn^{II}_4Mn^{III}_2O_2(O_2CCMe_3)_{10}(Me_3CCO_2H)_4]$ cluster with $KMnO_4$ in 1-methylimidazole.

The IR spectra of complexes **1** and **2** have strong and broad bands in the 1609–1546 and 1369–1357 cm^{-1} region, which are due to asymmetric and symmetric vibrations, respectively, of the coordinated carboxylate groups [29,30] of the pivalate ligand. The broad bands with medium intensity in the 3159–3067 cm^{-1} region can be ascribed to the absorption frequencies of the N–H vibration of Im and O–H vibration of solvate pivalic molecules in compound **1**.

Thermal analysis of **1** and **2** has been performed in a nitrogen atmosphere in the temperature range 25–600 °C. For **1** the first weight loss of 19.05% from 110 to 210 °C corresponds to the loss of a half molecule (per formula unit) of solvate pivalic acid, one molecule of the uncoordinated pivalic anion and one imidazole molecule (calculated 19.25%). On further heating, the decomposition of remaining organic ligands takes place in two unidentified steps with total weight loss of 61.08% and is completed below 500 °C to give the expected oxide (observed 19.95%, calculated 20.00%). It is interesting to note that the mixed-valent oxo-centered trinuclear compound **2** decomposes to the final products below 275 °C, a much lower temperature compared to the above mentioned homo-valent compound **1**. The first weight loss of about 4.54% occurred at 110 °C, which corresponds to the loss of a half molecule (per formula unit) of 1-MeIm (calculated 3.97%). A further weight loss of 30.25% occurred between 130 and 210 °C, which agrees with calculated values of 29.62% for the release of the remaining 1-MeIm molecules and one molecule of pivalate ligand. The decomposition of the pivalate ligands was completed at ca. 275 °C (the weight loss is 40.55%) with the observed remaining weight percentage of 24.58%.

3.2. Crystal structures

3.2.1. The structure of $[Mn_3O(O_2CCMe_3)_6(Im)_3](Me_3CCO_2)\cdot 0.5Me_3CCO_2H$ (1)

The crystal structure of **1** consists of two independent $[Mn_3O(O_2CCMe_3)_6(Im)_3]^+$ cations (molecules **A** and **B**), two $Me_3CCO_2^-$ anions and a neutral Me_3CCO_2H molecule (Fig. 1). The structure of cation **A** is shown in Fig. 2. Selected bond distances and angles for **1** are listed in Table 2. Three Mn(III) atoms form a nearly equilateral triangle with an oxygen atom in the center. The Mn···Mn distances within the triangle are all very similar (3.260 ± 0.006 Å). The central μ_3-oxygen atom is slightly displaced from the Mn_3 triangular plane (0.015(2) Å for molecule **A** and 0.019(2) Å for molecule **B**). The Mn–(μ_3-O) bond distances are in the range of 1.879(2)–1.890(2) Å (Table 2). Four oxygen atoms from the bridging carboxylate groups and a terminal imidazole nitrogen atom additionally complete coordination at each Mn(III) atom. The Mn–O_{carb} bond distances range from 1.923(2) to 2.186(3) Å, and the Mn–N bond distances lie in the range of 2.011(3)–2.026(3) Å. Thus, the manganese coordination geometry can be regarded as a slightly distorted octahedron. The configuration, bond distances and bond angles of molecules **A** and **B**

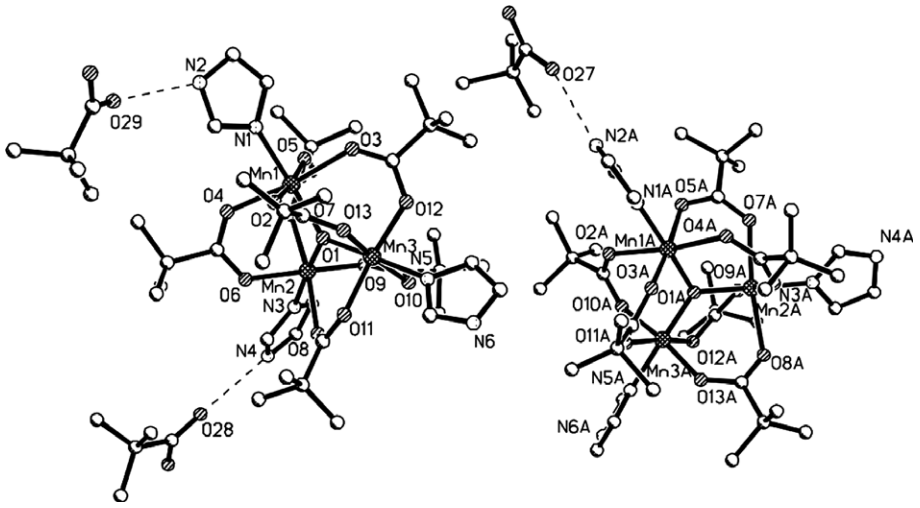

Fig. 1. View of the structure of complex **1** (molecule **A**, left; molecule **B**, right). Hydrogen bonds are shown as dashed lines. Hydrogen atoms are omitted for clarity.

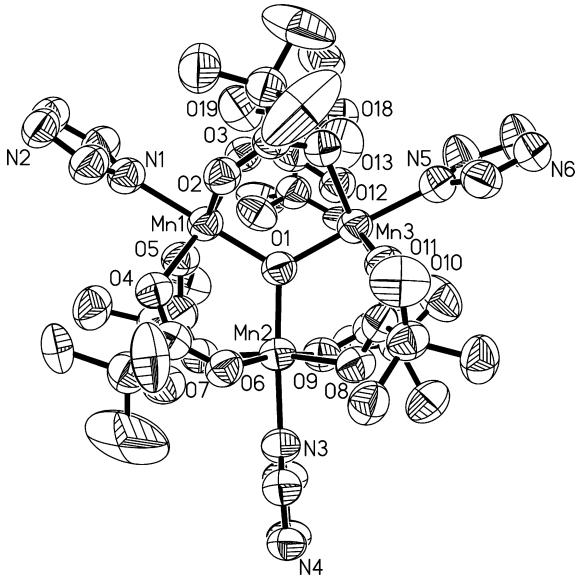

Fig. 2. View of the structure of molecule **A** in compound **1.** Hydrogen atoms are omitted for clarity.

are in a good agreement with the data in earlier investigated structures of oxo-centered trinuclear manganese(III) carboxylate complexes [13–15] (Table 3).

The presence of the uncoordinated carboxylic group of pivalic acid and the solvate acid molecule as well as of the N–H group of imidazole ligand results in an extensive hydrogen-bonded network in complex **1**. It is interesting to note that in this crystal structure the formation of centrosymmetric motifs consisting of four trinuclear clusters is observed. The packing of molecules in the crystal structure along the [0 0 1] direction is shown in Fig. 3a. In addition, these centrosymmetric motives are connected by hydrogen bonds N–H···O (2.636(4)–2.866(4) Å) between carboxyl oxygen atoms of pivalic acid and nitrogen atoms of Im, as well as by hydrogen bonds O–H···O of 2.556(4) Å, forming zig-zag chains (Fig. 3b). Finally, a 3D supramolecular architecture is formed in compound **1**. The parameters of all intermolecular hydrogen bonds are listed in Table 4.

*3.2.2. The structure of $[Mn_3O(O_2CCMe_3)_6(1\text{-}MeIm)_3]$ (**2**)*

X-ray diffraction analysis revealed that complex **2** consists of two independent molecules (**A** and **B**) of the trinuclear oxo-centered $[Mn_3O(O_2CCMe_3)_6(1\text{-}MeIm)_3]$ cluster in the unit cell. The structure of molecule **B** is shown in Fig. 4. Selected bond distances and angles for **2** are listed in Table 5. Each Mn atom adopts a slightly distorted octahedral geometry and is coordinated by an oxygen atom of the central triangle, four oxygen atoms from bridging pivalate ligands, and a terminal 1-MeIm nitrogen atom. The central μ_3-oxygen atom is slightly displaced from the Mn_3 triangular plane (0.029(2) Å for molecule **A** and 0.028(2) Å for molecule **B**). The Mn···Mn distances are in the range of 3.220(2)–3.408(2) Å, and the Mn(2)···Mn(3) distances of 3.220(2) and 3.312(2) Å for **A** and **B** molecules, respectively, are significantly shorter than the Mn(1)···Mn(2) (average value 3.391 Å) and Mn(1)···Mn(3) (average value 3.406 Å) distances. Based on the neutral charge of the $[Mn_3O(O_2CCMe_3)_6(1\text{-}MeIm)_3]$ cluster, the Mn oxidation states in this complex are given as $[Mn^{III}_2Mn^{II}O]^{6+}$. As expected for its lower oxidation state, the position of the Mn(II) atom can be assigned on the basis of its longer metal–μ-oxygen and metal–ligand bond distances compared with the Mn(III) atoms (Table 3). From these data Mn(1) is readily assigned as the Mn^{II} center, whereas Mn(2) and Mn(3) atoms are Mn^{III} centers. The Mn^{III}–O(1) bond distances are in the range 1.800(4)–1.848(4) Å, which is in agreement with the common basic carboxylate type seen for the above mentioned trinuclear manganese(III) complex **1** and other trinuclear manganese(III) carboxylate complexes (Table 3). For manganese(II) atoms these distances are significantly longer and

Table 2
Selected bond distances (Å) and angles (°) for compound **1**

Molecule	A	B	Molecule	A	B
Mn(1)–O(1)	1.885(2)	1.887(2)	Mn(2)–O(8)	2.182(2)	2.162(3)
Mn(1)–O(2)	1.944(2)	2.175(3)	Mn(2)–O(9)	1.935(2)	1.945(3)
Mn(1)–O(3)	2.173(2)	1.923(2)	Mn(2)–N(3)	2.011(3)	2.020(3)
Mn(1)–O(4)	2.165(2)	2.158(2)	Mn(3)–O(1)	1.890(2)	1.883(2)
Mn(1)–O(5)	1.925(2)	1.940(2)	Mn(3)–O(10)	2.171(2)	2.186(3)
Mn(1)–N(1)	2.013(3)	2.026(3)	Mn(3)–O(11)	1.931(2)	1.929(3)
Mn(2)–O(1)	1.879(2)	1.880(2)	Mn(3)–O(12)	1.927(2)	2.146(3)
Mn(2)–O(6)	1.947(2)	1.947(2)	Mn(3)–O(13)	2.143(2)	1.931(3)
Mn(2)–O(7)	2.174(2)	2.159(2)	Mn(3)–N(5)	2.023(3)	2.017(3)
O(1)–Mn(1)–O(2)	93.84(9)	92.49(9)	O(1)–Mn(2)–O(8)	92.06(9)	94.60(10)
O(1)–Mn(1)–O(5)	94.47(10)	94.58(10)	O(9)–Mn(2)–O(8)	98.75(9)	93.05(11)
O(5)–Mn(1)–O(2)	171.41(10)	84.82(9)	O(6)–Mn(2)–O(8)	84.51(9)	87.57(10)
O(1)–Mn(1)–N(1)	178.47(12)	178.15(11)	N(3)–Mn(2)–O(8)	85.39(10)	86.21(11)
O(5)–Mn(1)–N(1)	86.91(11)	86.06(11)	O(7)–Mn(2)–O(8)	172.21(9)	171.54(10)
O(2)–Mn(1)–N(1)	84.81(10)	85.84(11)	O(1)–Mn(3)–O(12)	94.07(9)	93.74(10)
O(1)–Mn(1)–O(4)	93.50(9)	94.53(9)	O(1)–Mn(3)–O(11)	93.82(9)	93.64(10)
O(5)–Mn(1)–O(4)	94.13(10)	92.14(10)	O(12)–Mn(3)–O(11)	172.08(10)	85.89(11)
O(2)–Mn(1)–O(4)	87.52(9)	172.55(9)	O(1)–Mn(3)–N(5)	177.70(10)	178.68(12)
N(1)–Mn(1)–O(4)	85.73(10)	87.17(11)	O(12)–Mn(3)–N(5)	86.28(11)	86.16(12)
O(1)–Mn(1)–O(3)	93.53(9)	94.40(10)	O(11)–Mn(3)–N(5)	85.86(11)	85.04(12)
O(5)–Mn(1)–O(3)	85.33(9)	170.81(10)	O(1)–Mn(3)–O(13)	94.80(9)	93.97(10)
O(2)–Mn(1)–O(3)	92.00(9)	96.74(10)	O(12)–Mn(3)–O(13)	91.61(9)	94.16(11)
N(1)–Mn(1)–O(3)	87.25(11)	85.02(11)	O(11)–Mn(3)–O(13)	87.07(9)	172.37(11)
O(4)–Mn(1)–O(3)	172.98(9)	85.21(10)	N(5)–Mn(3)–O(13)	87.46(10)	87.35(12)
O(1)–Mn(2)–O(9)	93.49(9)	93.71(10)	O(1)–Mn(3)–O(10)	93.27(9)	93.57(10)
O(1)–Mn(2)–O(6)	95.86(9)	94.14(10)	O(12)–Mn(3)–O(10)	85.70(9)	172.49(10)
O(9)–Mn(2)–O(6)	169.98(10)	172.06(10)	O(11)–Mn(3)–O(10)	94.51(9)	95.35(11)
O(1)–Mn(2)–N(3)	176.85(11)	179.16(11)	N(5)–Mn(3)–O(10)	84.48(10)	86.57(12)
O(9)–Mn(2)–N(3)	85.09(10)	85.99(11)	O(13)–Mn(3)–O(10)	171.67(9)	83.62(11)
O(6)–Mn(2)–N(3)	85.75(10)	86.15(11)	Mn(2)–O(1)–Mn(1)	120.01(11)	120.24(11)
O(1)–Mn(2)–O(7)	94.46(9)	93.73(9)	Mn(2)–O(1)–Mn(3)	120.18(11)	119.67(12)
O(9)–Mn(2)–O(7)	85.11(10)	87.88(10)	Mn(1)–O(1)–Mn(3)	119.79(11)	120.06(12)
O(6)–Mn(2)–O(7)	90.55(9)	90.36(10)			
N(3)–Mn(2)–O(7)	88.22(10)	85.47(10)			

equal to 2.128(5) Å for Mn(1)–O(1) and 2.170(4) Å for Mn(1A)–O(1A). The four Mn–O_{carb} distances around manganese(III) atoms are in the range of 1.947(5)–2.174(5) Å, and the Mn^{III}–N distances (2.060(6)–2.064(5) Å) are quite similar to those found in **1**. As expected for a typical manganese(II) atom, Mn–O_{carb} bond distances are found in the range of 2.129(5)–2.207(5) Å, which is slightly longer than those for Mn^{III} atoms. The Mn^{II}–N distance of 2.251(6) Å at Mn(1) and Mn(1A) is also longer than that for the trivalent manganese atom (2.256(6) Å). The Mn–O(1)–Mn angles range from 116.6(2)° up to 125.4(2)° and differ slightly from the analogous angles which were found in a Mn_3O cluster with imposed C_2 symmetry [9].

In contrast to **1**, in which an extensive network of hydrogen-bonding interactions is observed due to the presence of the uncoordinated carboxyl group of pivalic acid and the NH group of imidazole, aromatic C–H$\cdots\pi$ interactions [31–33] embracing 1-methylimidazole rings enhance the structural stability in compound **2**. Because the 1-MeIm heterocycles are not all parallel with each other, the aromatic–aromatic interactions in compound **2** are either edge-to-face interactions or T-shaped orientations. In addition to the aromatic C–H$\cdots\pi$ interactions, five 1-MeIm heterocycles from six heterocycles (heterocycles are marked as follows: N1 ∩ N2 is cycle N1C1N2C2C3, N3 ∩ N4–N3C5N4C6C7, etc.) exhibit five contacts, each between aliphatic C–H of the methyl group and the π-cycle of another molecule (Table 6). Note that all six 1-MeIm heterocycles are involved in such interactions forming a 3D network in compound **2** (Fig. 5). The heterocycle N5A ∩ N6A forms with the N1A ∩ N2A heterocycle two types of C–H$\cdots\pi$ contacts, one exhibiting aromatic–aromatic edge-to-face interaction having a centroid–centroid distance of 4.468 Å and plane angle of 24.47° between the aromatic heterocycles, and the other being an aliphatic–aromatic interaction between the hydrogen (H12E) of the methyl group (C12) and imidazole cycle (N1A ∩ N2A) with the shortest interatomic distance of 2.835 Å. Further, the cycle N1A ∩ N2A interacts with N1 ∩ N2 forming an edge-to-face contact with the centroid–centroid distance of 4.242 Å (plane angle 31.69°) and the aliphatic–aromatic interaction of 3.032 Å (a typical aliphatic–aromatic interaction is in the range of 2.79–3.05 Å [32]). The third edge-to-face interaction is found between cycles N1 ∩ N2 and N5 ∩ N6 (centroid–centroid distance 4.374 Å, plane angle 24.22°) and there is

Table 3
Selected average bond distances (Å) in $[Mn_3O(O_2CCR)(L)_3]^{0,1+}$

Compound	Mn–μ-O	Mn–O_{carb}	Mn–L	Ref.
Mn^{III}_3O				
$[Mn_3O(O_2CCMe_3)_6(Py)_3]ClO_4 \cdot MeCN$	1.891	2.033	2.084 (Mn–N)	[13]
$[Mn_3O(O_2CMe)_6(3\text{-}MePy)_3]ClO_4$	1.900	2.002	2.101 (Mn–N)	[14]
$[Mn_3O(O_2CC_2H_5)_6(3\text{-}MePy)_3]ClO_4$	1.888	1.990	2.062 (Mn–N)	[14]
$[Mn_3O(O_2CC_3H_7)_6(Py)_3]ClO_4$	1.893	2.025	2.15 (Mn–N)	[15]
$[Mn_3O(O_2CCMe_3)_6(Im)_3](Me_3CCO_2) \cdot 0.5Me_3CCO_2H$	1.884	2.051	2.018 (Mn–N)	this work
$Mn^{III}_2Mn^{II}O$				
$[Mn_3O(O_2CMe)_6(Py)_3] \cdot Py$	1.936	2.105	2.167	[4,6]
$[Mn_3O(O_2CMe)_6(3\text{-}ClPy)_3]$	2.034 (Mn^{II})	2.114 (Mn^{II})	2.280 (Mn^{II}–N)	[5]
	1.863 (Mn^{III})	2.072 (Mn^{III})	2.143 (Mn^{III}–N)	
$[Mn_3O(O_2CPh)_6(Py)_2(H_2O)] \cdot 0.5MeCN$	2.135 (Mn^{II})	2.166 (Mn^{II})	2.237 (Mn^{II}–O)	[6]
	1.816 (Mn^{III})	2.072 (Mn^{III})	2.088 (Mn^{III}–N)	
$[Mn_3O(O_2CPh)_6(Py)_3] \cdot 2MeCN$	1.972 and 1.966 (Mn^{II} and Mn^{III})*	2.108 and 2.129 (Mn^{II} and Mn^{III})*	2.194 and 2.199 (Mn^{II} and Mn^{III})*	[12]
	1.819 (Mn^{III})	2.066 (Mn^{III})	2.077 (Mn^{III}–N)	
$[Mn_3O(O_2CPh\text{-}2F)_6(Py)_3] \cdot 2MeCN$	1.990 (Mn^{II})	2.109 (Mn^{II})	2.234 (Mn^{II}–N)	[11]
	1.871 (Mn^{III})	2.048 (Mn^{III})	2.118 (Mn^{III}–N)	
$[Mn_3O(O_2CPh\text{-}3Cl)_6(Py)_2(H_2O)] \cdot 0.5H_2O$	2.064 (Mn^{II})	2.054 (Mn^{II})	2.123 (Mn^{II}–O)	[11]
	1.833 (Mn^{III})	2.016 (Mn^{III})	2.061 (Mn^{III}–N)	
$[Mn_3O(O_2CPh\text{-}3Br)_6(Py)_2(H_2O)] \cdot \frac{1}{4}H_2O$	2.066 (Mn^{II})	2.036 (Mn^{II})	2.140 (Mn^{II}–O)	[11]
	1.827 (Mn^{III})	2.077 (Mn^{III})	2.083 (Mn^{III}–N)	
$[Mn_3O(O_2CCH_2Cl)_6(Py)_2(H_2O)] \cdot 0.5MeCN$	2.136 (Mn^{II})	2.171 (Mn^{II})	2.222 (Mn^{II}–O)	[17]
	1.805 (Mn^{III})	2.073 (Mn^{III})	2.064 (Mn^{III}–N)	
$[Mn_3O(O_2CCCl_3)_6(H_2O)_3]$	1.924	2.055		[18]
$[Mn_3O(O_2CCMe_3)_6(Py)_3]$	2.171 (Mn^{II})	2.172 (Mn^{II})	2.339 (Mn^{II}–N)	[13]
	1.830 (Mn^{III})	2.088 (Mn^{III})	2.107 (Mn^{III}–N)	
$[Mn_3O(O_2CCMe_3)_6(Py)_3]$	2.114 (Mn^{II})	2.165 (Mn^{II})	2.289 (Mn^{II}–N)	[19]
	1.818 (Mn^{III})	2.056 (Mn^{III})	2.099 (Mn^{III}–N)	
$[Mn_3O(O_2CCMe_3)_6(1\text{-}MeIm)_3]$	2.149 (Mn^{II})	2.163 (Mn^{II})	2.254 (Mn^{II}–N)	this work
	1.816 (Mn^{III})	2.056 (Mn^{III})	2.062 (Mn^{III}–N)	

a contact with 2.848 Å distance formed by the C–H of the methyl group (C12) and the π-cycle (Table 6). The next C–H···π interactions consisting of the edge-to-face contact (centroid–centroid distance 4.250 Å, plane angle 18.11°) and aliphatic–aromatic contact (2.952 Å) are found between N5 ∩ N6 and N3 ∩ N4 heterocycles. There is further close C–H···π contact with distance of 2.999 Å between heterocycle N3 ∩ N4 (C6) and N3A ∩ N4A (C7–H7A), which is probably more of a T-shaped interaction based on the interplane angle of 68.64°. It is noted that there is only the aliphatic–aromatic C–H···π interaction of 2.986 Å between the heterocycle N3A ∩ N4A and the neighboring heterocycle N5A ∩ N6A (the centroid–centroid distance is 5.953 Å and plane 86.72°).

3.3. Magnetic properties

The magnetic susceptibility χ_{Mol} between 1.9 and 300 K of the trinuclear, μ_3-oxo-bridged manganese(III) compound **1** was determined. In Fig. 6, the temperature dependence of the inverse molar susceptibility χ^{-1}_{Mol} is depicted. Above 55 K, the data can be fitted to the Curie–Weiss expression with a Weiss constant $\theta = -147$ K which is indicative of antiferromagnetic exchange interactions. The thermal dependence of the molar susceptibility, plotted as $\chi_{Mol}T$ versus T is shown in Fig. 7. The $\chi_{Mol}T$ value at 300 K is 8.14 emu K mol^{-1}, which is a little below the calculated value of 9 emu K mol^{-1} for three non-interacting manganese(III) ions ($S = 2$, $g = 2$). The decrease of $\chi_{Mol}T$ with decreasing temperature suggests overall antiferromagnetic exchange interactions. A simulation based on the model proposed by Borrás-Almenar et al. [25] using the isotropic Heisenberg–Dirac–Van Vleck term, $\widehat{H}_O = -2\Sigma_{i,f}J_{if}\widehat{S}_i\widehat{S}_f$, as the leading part of the exchange spin Hamiltonian, was applied. Thereby and in correspondence with the structural data, the compound is regarded as an isosceles triangle and consequently, two different exchange coupling constants are considered: J between Mn(3)–Mn(1) and Mn(3)–Mn(2) and J^* between Mn(1) and Mn(2). However, as shown in a theoretical study by Brechin et al. [34], there is a high density of different energy levels close to the ground state and also the total S value of the ground state depends strongly on the ratio J/J^*, hence it is a quite complex situation. Taking the data of the temperature dependence of the magnetic susceptibility and the magnetization data which are measured at 1.85 K (Figs. 7 and S1), a simulation of the experimental data revealed the following parameters: $J = -7.5\ cm^{-1}$, $J^* = -5.2\ cm^{-1}$, $D = 15.5\ cm^{-1}$ and $g = 2.1$. With these parameters, the $\chi_{Mol}T$ versus T data can be simulated fairly well. On the basis of the same parameter set, also the magnetization data can be approached reasonably well,

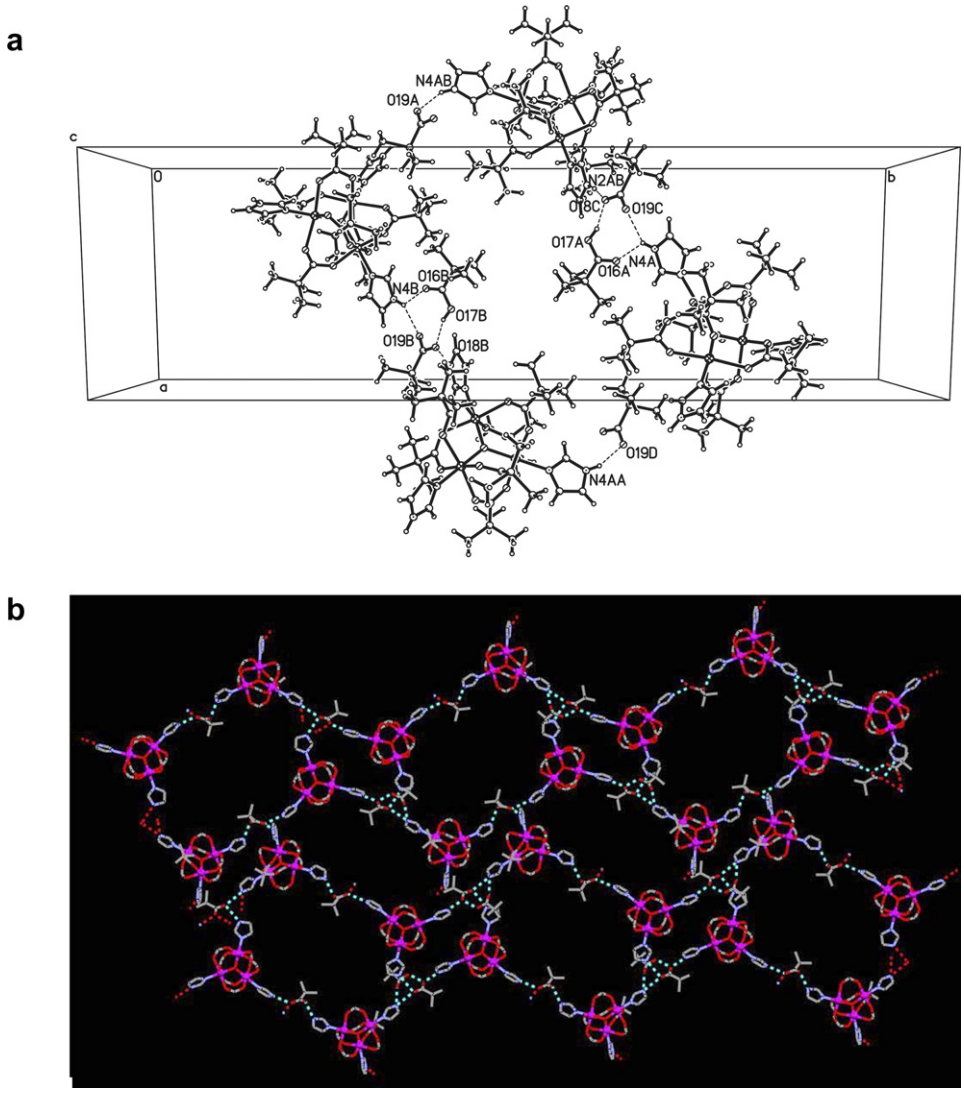

Fig. 3. (a) A fragment of the crystal structure in compound **1.** Hydrogen bonds are shown as dashed lines. (b) Perspective view of the crystal structure along the *b* axis. Hydrogen bonds are shown as dashed lines, the methyl groups of the coordinated pivalic acid are omitted for clarity.

especially if one notes the complex configuration of multiple states lying close to the ground-state. Overall, a ground state with $S = 0$ but with energetically close lying states with $S = 1$ and $S = 2$ can be anticipated.

Table 4
Hydrogen bonding interactions in compound **1**

D–H...A	*d*(D–H) (Å)	*d*(H...A) (Å)	*d*(D...A) (Å)	∠(DHA)
N(2)–H(2)...O(14)	0.88	1.96	2.685(5)	139.3
N(2A)–H(2A)...O(18)[1]	0.88	1.86	2.730(4)	169.4
N(4)–H(4)...O(19)[2]	0.88	2.13	2.779(4)	130.3
N(4)–H(4)...O(16)	0.88	2.22	2.866(4)	130.4
N(4A)–H(4A)...O(19)[3]	0.88	1.90	2.733(4)	156.2
N(6)–H(6)...O(15)[2]	0.88	1.80	2.655(4)	164.2
N(6A)–H(6A)...O(15)[2]	0.88	1.78	2.636(4)	164.1
O(17)–H(17)...O(18)[2]	0.84	1.75	2.556(4)	159.0

Symmetry transformations: [1]$x - 1, y, z$; [2]$x + 1/2, -y + 1/2, z + 1/2$; [3]$-x + 1, -y + 1, -z + 1$.

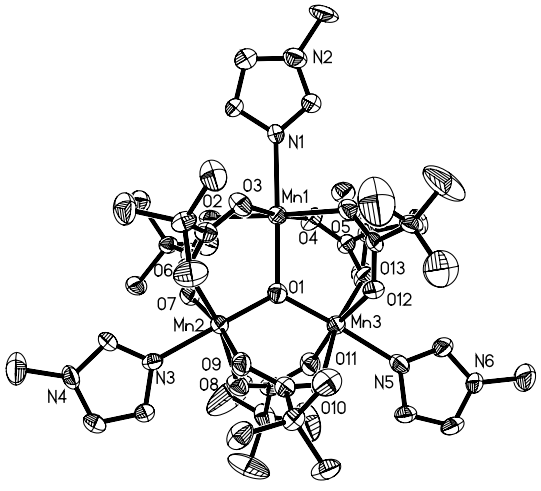

Fig. 4. View of the structure of molecule **B** in compound **2**. Hydrogen atoms are omitted for clarity.

Table 5
Selected bond distances (Å) and angles (°) for compound **2**

Molecule	A	B	Molecule	A	B
Mn(1)–O(1)	2.128(5)	2.170(4)	Mn(2)–O(8)	2.174(5)	2.090(5)
Mn(1)–O(2)	2.174(4)	2.178(5)	Mn(2)–O(9)	1.968(5)	2.030(5)
Mn(1)–O(3)	2.143(5)	2.149(5)	Mn(2)–N(3)	2.064(5)	2.063(6)
Mn(1)–O(4)	2.129(5)	2.143(5)	Mn(3)–O(1)	1.848(4)	1.813(4)
Mn(1)–O(5)	2.178(5)	2.207(5)	Mn(3)–O(10)	2.173(4)	2.110(5)
Mn(1)–N(1)	2.251(6)	2.256(6)	Mn(3)–O(11)	1.985(5)	2.000(5)
Mn(2)–O(1)	1.803(5)	1.800(4)	Mn(3)–O(12)	2.003(4)	2.047(5)
Mn(2)–O(6)	2.133(5)	1.998(5)	Mn(3)–O(13)	2.136(5)	2.015(5)
Mn(2)–O(7)	1.947(5)	2.082(6)	Mn(3)–N(5)	2.061(6)	2.060(6)
O(1)–Mn(1)–O(2)	91.13(17)	94.05(17)	O(1)–Mn(2)–O(8)	95.47(19)	94.15(19)
O(1)–Mn(1)–O(5)	90.92(17)	91.51(18)	O(9)–Mn(2)–O(8)	90.01(18)	92.3(2)
O(2)–Mn(1)–O(5)	177.60(17)	174.36(19)	O(6)–Mn(2)–O(8)	168.50(17)	86.4(2)
O(1)–Mn(1)–N(1)	176.90(17)	174.01(18)	N(3)–Mn(2)–O(8)	84.25(19)	86.0(2)
O(1)–Mn(1)–O(3)	92.47(17)	89.70(17)	O(7)–Mn(2)–O(8)	86.98(18)	170.24(19)
O(5)–Mn(1)–N(1)	91.40(19)	84.2(2)	O(1)–Mn(3)–O(12)	94.2(2)	96.69(19)
O(4)–Mn(1)–O(1)	91.90(18)	94.35(18)	O(1)–Mn(3)–O(11)	94.7(2)	95.00(19)
O(4)–Mn(1)–O(5)	90.95(19)	93.9(2)	O(11)–Mn(3)–O(12)	171.0(2)	88.9(2)
O(4)–Mn(1)–O(2)	87.73(18)	84.8(2)	O(1)–Mn(3)–N(5)	176.0(2)	178.8(2)
O(4)–Mn(1)–N(1)	86.0(2)	90.1(2)	O(12)–Mn(3)–N(5)	86.0(2)	84.5(2)
O(3)–Mn(1)–O(5)	88.22(18)	88.1(2)	O(11)–Mn(3)–N(5)	85.1(2)	85.3(2)
O(3)–Mn(1)–O(2)	92.94(18)	92.9(2)	O(1)–Mn(3)–O(13)	99.00(18)	95.6(2)
O(3)–Mn(1)–N(1)	89.7(2)	86.0(2)	O(12)–Mn(3)–O(13)	91.63(18)	92.2(2)
O(2)–Mn(1)–N(1)	86.51(18)	90.4(2)	O(11)–Mn(3)–O(13)	88.70(18)	169.1(2)
O(4)–Mn(1)–O(3)	175.57(19)	175.5(2)	N(5)–Mn(3)–O(13)	85.02(19)	84.0(2)
O(1)–Mn(2)–O(9)	94.89(19)	94.33(19)	O(1)–Mn(3)–O(10)	92.87(18)	94.4(2)
O(1)–Mn(2)–O(6)	95.97(19)	95.81(19)	O(12)–Mn(3)–O(10)	86.72(17)	168.8(2)
O(9)–Mn(2)–O(6)	87.90(18)	169.84(18)	O(11)–Mn(3)–O(10)	91.10(18)	89.1(2)
O(1)–Mn(2)–N(3)	179.5(2)	179.8(2)	N(5)–Mn(3)–O(10)	83.12(19)	84.4(2)
O(9)–Mn(2)–N(3)	84.65(19)	85.6(2)	O(13)–Mn(3)–O(10)	168.11(18)	87.6(2)
N(3)–Mn(2)–O(6)	84.30(19)	84.30(19)			
O(1)–Mn(2)–O(7)	95.06(19)	95.50(19)	Mn(2)–O(1)–Mn(1)	118.4(2)	117.9(2)
O(7)–Mn(2)–O(9)	169.83(18)	85.6(2)	Mn(2)–O(1)–Mn(3)	124.1(3)	125.4(2)
O(7)–Mn(2)–O(6)	93.12(18)	94.1(2)	Mn(3)–O(1)–Mn(1)	117.4(2)	116.6(2)
O(7)–Mn(2)–N(3)	85.38(19)	84.4(2)			

Table 6
CH···π contacts in compound **2**

Heterocycle···heterocycle[a]	Aliphatic CH···π (Å) (θ(HCC′), °)		Aromatic CH···π (Å) (θ (HCC′), °)		Centroid–centroid distance (Å) (plane angle, °)
N5A ∩ N6A···N1A ∩ N2A	C12A–H12E···C3A[b]	2.835 (36.25)			4.468 (24.47)
N1A ∩ N2A···N1 ∩ N2	C4–H4A···C3A[c]	3.032 (41.42)	C2A–H2A···C1[g]	2.917 (55.92)	4.242 (31.69)
N1 ∩ N2···N5 ∩ N6	C12–H12A···C3[d]	2.848 (29.68)			4.374 (24.22)
N5 ∩ N6···N3 ∩ N4	C8–H8A···C11[e]	2.952 (29.34)			4.250 (18.11)
N3 ∩ N4···N3A ∩ N4A			C7A–H7A···C6[h]	2.999 (45.85)	4.873 (68.64)
N3A ∩ N4A···N5A ∩ N6A	C8A–H8D···C9A[f]	2.986 (21.53)			

[a] Heterocycle N1 ∩ N2 (N1, C1, N2, C2, C3); N3 ∩ N4 (N3, C5, N4, C6, C7); N5 ∩ N6 (N5, C9, N6, C10, C11); N1A ∩ N2A (N1A, C1A, N2A, C2A, C3A); N3A ∩ N4A (N3A, C5A, N4A, C6A, C7A); N5A ∩ N6A (N5A, C9A, N6A, C10A, C11A).
[b] $1 - x, 1/2 + y, 1 - z$.
[c] $1 - x, y, z$.
[d] $-x, 1/2 + y, 1 - z$.
[e] $-x, -1/2 + y, 2 - z$.
[f] $1 - x, -3/2 + y, -z$.
[g] $1 + x, y, z$.
[h] $x, y, -1 + z$.

For the trinuclear mixed-valence compound **2**, the temperature dependence of the inverse molar susceptibility χ_{Mol}^{-1} between 1.9 and 300 K is depicted in Fig. 8. A fit above 55 K of the data to the Curie–Weiss expression gives a Weiss constant $\theta = -140$ K, which is indicative of antiferromagnetic exchange interactions. In Fig. 9 the thermal dependence of the molar susceptibility, plotted as $\chi_{\mathrm{Mol}}T$ versus T, is shown. The experimentally determined room

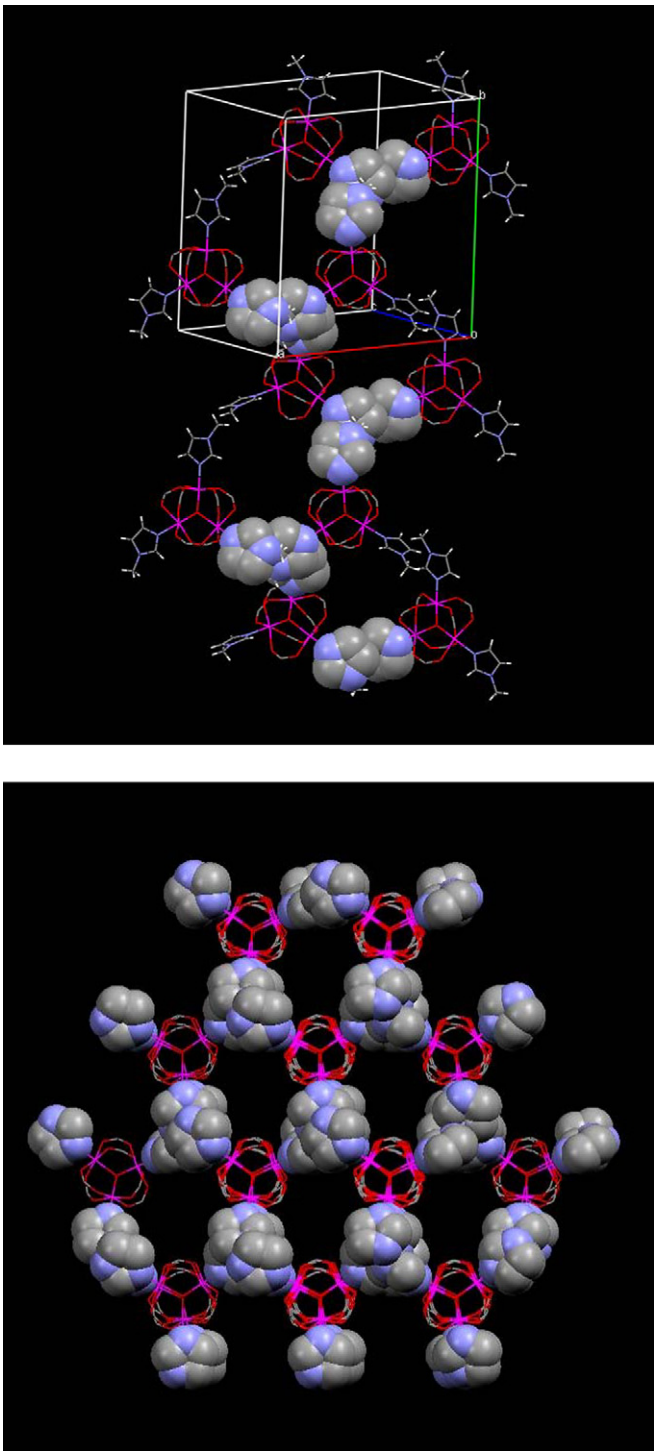

Fig. 5. Molecular packing and aromatic–aromatic interactions of compound **2**. The edge-to-face contacts are highlighted with the space-filled 1-MeIm heterocycle. The methyl groups of pivalic acid are omitted for clarity.

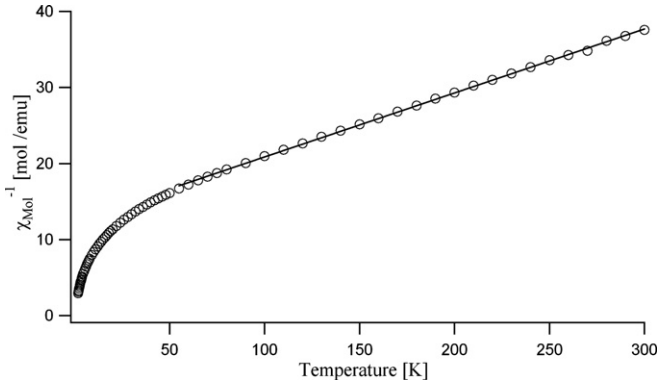

Fig. 6. The inverse molar susceptibility χ_{Mol}^{-1} vs. T for compound **1**. The solid line represents a linear fit to the data from 55 to 300 K, giving a Weiss constant $\theta = -147$ K.

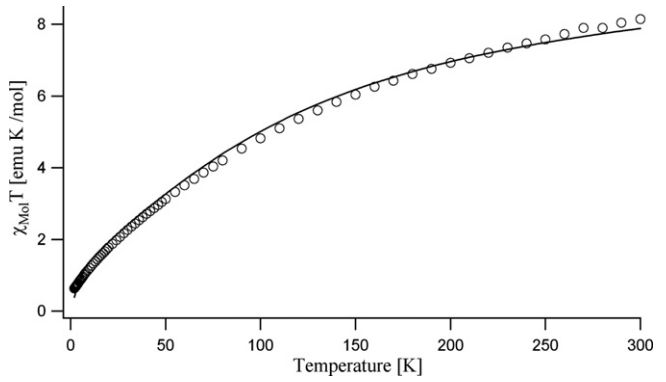

Fig. 7. Plot of the $\chi_{Mol}T$ product vs. T of compound **1** in an applied field of 1 kG. The solid curve represents a simulation from 2 to 300 K with the parameters $J = -7.5\ \text{cm}^{-1}$, $J^* = -5.2\ \text{cm}^{-1}$, $D = 15.5\ \text{cm}^{-1}$ and $g = 2.1$ (see text).

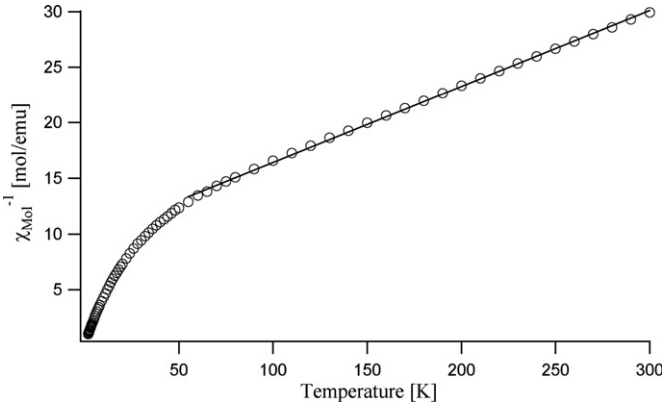

Fig. 8. The inverse molar susceptibility χ_{Mol}^{-1} vs. T for compound **2**. The solid line represents a linear fit to the data from 55 to 300 K, giving a Weiss constant $\theta = -140$ K.

temperature value $\chi_{Mol}T$ of 10.0 emu K mol^{-1} is in good agreement with a calculated value of 10.38 emu K mol^{-1} for the non-interacting two manganese(III) ions ($S = 2$, $g = 2$) and one manganese(II) ion ($S = 5/2$, $g = 2$). With decreasing temperature the $\chi_{Mol}T$ values drop slowly, which suggests overall antiferromagnetic exchange interactions. For the simulation of the data [25], two different exchange interactions have been considered: J between the Mn(II) ($S = 5/2$) and the two Mn(III) ($S = 2$) centers, and J^* between the two Mn(III) centers. The parameters found for the best simulation of the experimental data

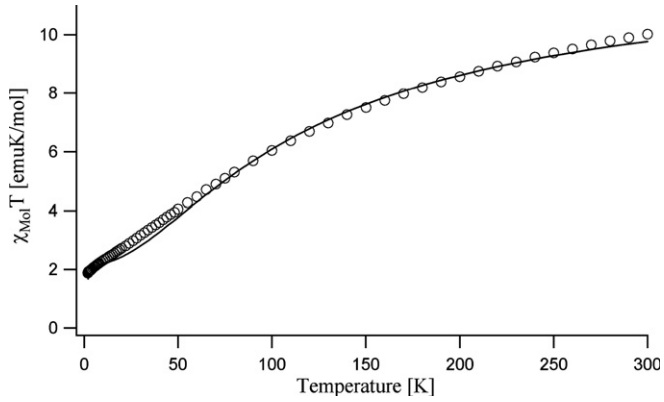

Fig. 9. Plot of the $\chi_{Mol}T$ product vs. T of compound **2** in an applied field of 1 kG. The solid curve represents the fit from 2 to 300 K with the parameters $J = -7.0\ cm^{-1}$, $J^* = -1.6\ cm^{-1}$, $D = -1.6\ cm^{-1}$ and $g = 2.2$ (see text).

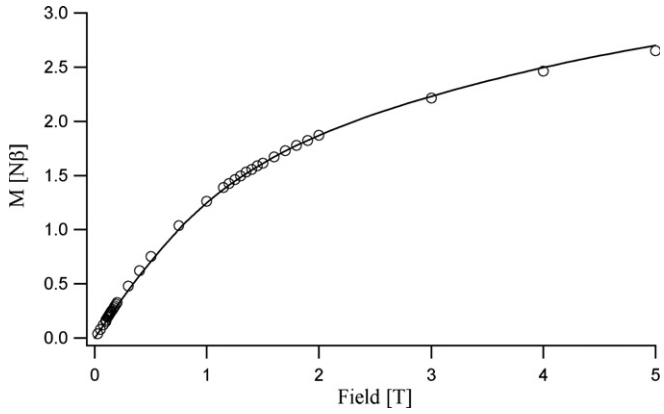

Fig. 10. Field dependence of the magnetization of compound **2** measured at $T = 1.85$ K. The solid curve represents the fit with the parameters $J = -7.0\ cm^{-1}$, $J^* = -1.6\ cm^{-1}$, $D = -1.6\ cm^{-1}$ and $g = 2.2$ (see text).

are: $J = -7.0\ cm^{-1}$, $J^* = -1.6\ cm^{-1}$, $D = -1.6\ cm^{-1}$ and $g = 2.2$. Moreover, with the same parameter set, a fairly good simulation of the magnetization data, measured at 1.85 K (see Fig. 10), has been obtained. At a magnetic field of 5 T, M_{sat} is not yet reached but a value close to 3 Nβ can be estimated. Accordingly, this would be consistent with a total ground state spin value of $S = 3/2$. This result is in accordance with a related detailed study by Ribas et al. [11].

4. Conclusions

In summary, we have synthesized and structurally characterized two new μ-oxo trinuclear manganese carboxylate complexes with imidazole and 1-methylimidazole ligands. One of them, complex $[Mn_3O(O_2CCMe_3)_6(Im)_3](Me_3CCO_2) \cdot 0.5Me_3CCO_2H$ (**1**) is a homo-valent Mn^{III}_3O cluster, which has been synthesized by comproportionation reaction of manganese(II) chloride with $KMnO_4$, imidazole and an excess of pivalic acid, whereas complex $[Mn_3O(O_2CCMe_3)_6(1\text{-}MeIm)_3]$ (**2**), which is a mixed-valent $Mn^{III}_2Mn^{II}O$ cluster, was isolated by the reaction of hexanuclear mixed-valent $[Mn^{III}_4Mn^{III}_2O_2(O_2CCMe_3)_{10}(Me_3CCO_2H)_4]$ with $KMnO_4$ in 1-methylimidazole. The trinuclear nature of these complexes has been compared to that of the previously reported μ-oxo trinuclear manganese carboxylates. The magnetic properties of **1** and **2** were studied by variable-temperature susceptibility measurements. The results reveal that both compounds are antiferromagnetically coupled, spin-frustrated triangular systems exhibiting weak to moderate exchange coupling constants.

Acknowledgment

This work was supported by the Swiss National Science Foundation (SCOPES 7MDPJ065712.01/1 and IB7320-110976/1).

Appendix A. Supplementary data

Crystallographic data have been deposited with the Cambridge Crystallographic Data Centre, CCDC Nos. 295955 (**1**), 295956 (**2**). Copies of this information may be obtained from The Director, CCDC, 12 Union Road, Cambridge, CB2 1EZ, UK (fax: +44 1233 336 033; e-mail: deposit@ccdc.cam.ac.uk or www: http://www.ccdc.cam.ac.uk). Supplementary data associated with this article can be found, in the online version, at doi:10.1016/j.poly.2006.07.014.

References

[1] (a) W. Wernsdorfer, N.E. Chakov, G. Christou, Phys. Rev. B 70 (2004) 132413;
(b) A.J. Tasiopoulos, W. Wernsdorfer, K.A. Abboud, G. Christou, Angew. Chem. Int. Ed. 43 (2004) 6338;
(c) A.J. Tasiopoulos, A. Vinslava, W. Wernsdorfer, K.A. Abboud, G. Christou, Angew. Chem. Int. Ed. 43 (2004) 2117;
(d) N. Aliaga-Alcalde, R.S. Edwards, S.O. Hill, W. Wernsdorfer, K. Folting, G. Christou, J. Am. Chem. Soc. 126 (2004) 12503;
(e) G. Rajaraman, M. Murugesu, E.C. Sañudo, M. Soler, W. Wernsdorfer, M. Helliwell, C. Muryn, J. Raftery, S.J. Teat, G. Christou, E.K. Brechin, J. Am. Chem. Soc. 47 (2004) 15445;
(f) M. Murugesu, J. Raftery, W. Wernsdorfer, G. Christou, E.K. Brechin, Inorg. Chem. 43 (2004) 4203;
(g) M. Murugesu, M. Habrych, W. Wernsdorfer, K.A. Abboud, G. Christou, J. Am. Chem. Soc. 126 (2004) 4766;
(h) G. Christou, Polyhedron 24 (2005) 2065.
[2] (a) L. Que Jr., A.E. True, Prog. Inorg. Chem. 38 (1990) 97;
(b) V.L. Pecoraro, Manganese Redox Enzymes, VCH Publishers Inc., New York, 1992;
(c) G.C. Dismukes, Chem. Rev. 96 (1996) 2909;
(d) G. Christou, Acc. Chem. Res. 22 (1989) 328.
[3] S. Uemura, A. Spencer, G. Wilkinson, J. Chem. Soc., Dalton Trans. (1973) 2565.
[4] A.R.E. Baikie, M.B. Hursthouse, D.B. New, P. Thornton, J. Chem. Soc., Chem. Commun. (1978) 62.
[5] A.R.E. Baikie, M.B. Hursthouse, L. New, P. Thornton, R.G. White, J. Chem. Soc., Chem. Commun. (1980) 684.
[6] J.B. Vincent, H.R. Chang, K. Folting, J.C. Huffman, G. Christou, D.N. Hendrickson, J. Am. Chem. Soc. 109 (1987) 5703.
[7] H.G. Jang, J.B. Vincent, M. Nakano, J.C. Huffman, G. Christou, M. Sorai, R.J. Wittebort, D.N. Hendrickson, J. Am. Chem. Soc. 111 (1989) 7778.

[8] M. Nakano, M. Sorai, J.B. Vincent, G. Christou, H.G. Jang, D.N. Hendrickson, Inorg. Chem. 28 (1989) 4608.
[9] J.K. Mccusker, H.G. Jang, S. Wang, G. Christou, D.N. Hendrickson, Inorg. Chem. 31 (1992) 1874.
[10] S.W. Zhang, Y.G. Wei, Q. Liu, M.C. Shao, Polyhedron 15 (1996) 1014.
[11] J. Ribas, B. Albela, H. Stoeckli-Evans, G. Christou, Inorg. Chem. 36 (1997) 2352.
[12] Z.J. Zhong, J.-Q. Tao, H. Li, X.-Z. You, T.C.W. Mak, Polyhedron 16 (1997) 1719.
[13] R.W. Wu, M. Poyraz, F.E. Sowrey, C.E. Anson, S. Wocadle, A.K. Powell, U.A. Jayasooriya, R.D. Cannon, T. Nakamoto, M. Katada, H. Sano, Inorg. Chem. 37 (1998) 1913.
[14] J. An, Z.-D. Chen, J. Bian, X.-L. Jin, S.-X. Wang, G.-X. Xu, Inorg. Chim. Acta 287 (1999) 82.
[15] J. Li, S. Yang, F. Zhang, Z. Tang, S. Ma, Q. Shi, Q. Wu, Z. Huang, Inorg. Chim. Acta 294 (1999) 109.
[16] C. Canada-Vilalta, J.C. Huffman, W.E. Streib, E.R. Davidson, G. Christou, Polyhedron 20 (2001) 1375.
[17] J. Li, F. Zhang, Q. Shi, J. Wang, Yu. Wang, Z. Zhou, Inorg. Chem. Commun. 5 (2002) 51.
[18] J. Kim, H. Cho, Inorg. Chem. Commun. 7 (2004) 122.
[19] N.V. Gerbeleu, G.A. Timco, O.S. Manole, Y.T. Struchkov, A.S. Batsanov, S.V. Grebenco, Russ. J. Coord. Chem. 20 (1994) 357.
[20] N.V. Gerbeleu, A.S. Batsanov, G.A. Timco, Yu.T. Struchkov, K.M. Indrichan, G.A. Popovici, Dokl. Akad. Nauk SSSR 294 (1987) 878.
[21] A.S. Batsanov, Y.T. Struchkov, G.A. Timco, N.V. Gerbeleu, O.S. Manole, S.V. Grebenco, Russ. J. Coord. Chem. 20 (1994) 604.
[22] A.R.E. Baikie, A.J. Howes, M.B. Hursthouse, A.B. Quick, P. Thornton, J. Chem. Soc., Chem. Commun. 4 (1986) 1587.
[23] G.M. Sheldrick, Acta Crystallogr., Sect. A 46 (1998) 467.
[24] G.M. Sheldrick, SHELXS-97, University of Göttingen, Germany, 1999.
[25] J.J. Borrás-Almenar, J.M. Clemente-Juan, E. Coronado, B.S. Tsukerblat, Inorg. Chem. 38 (1999) 6081.
[26] T. Lis, Acta Crystallogr., Sect. B 36 (1980) 2042.
[27] G. Aromi, S.M.J. Aubin, M.A. Bolcar, G. Christou, H.J. Eppley, K. Folting, D.N. Hendrickson, J.C. Huffman, R.C. Squire, H.-L. Tsai, S. Wang, M.W. Wemple, Polyhedron 17 (1998) 3005.
[28] (a) M. Soler, E. Rumberger, K. Folting, D.N. Hendrickson, G. Christou, Polyhedron 20 (2001) 1365;
(b) M. Soler, W. Wernsdorfer, K. Folting, M. Pink, G. Christou, J. Am. Chem. Soc. 126 (2004) 2156.
[29] K. Nakamoto, Infrared and Raman Spectra of Inorganic and Coordination Compounds, Wiley, New York, 1986, p. 230.
[30] R.C. Mehrota, R. Bohra, Metal Carboxylates, Academic Press, New York, 1983, p. 47.
[31] C.A. Hunter, K.R. Lawson, J. Perkins, C.J. Urch, J. Chem. Soc., Perkin Trans. 2 (2001) 651.
[32] H. Suezawa, T. Yoshida, M. Hirota, H. Takahashi, Y. Umezawa, K. Honda, S. Tsuboyama, M. Nishio, J. Chem. Soc., Perkin Trans. 2 (2001) 2053.
[33] M. Nishio, Cryst. Eng. Commun. 6 (2004) 130.
[34] L.F. Jones, G. Rajaraman, J. Brockman, M. Murugesu, E.C. Sanudo, J. Raftery, S.J. Teat, W. Wernsdorfer, G. Christou, E.K. Brechin, D. Collison, Chem. Eur. J. 10 (2004) 5180.